

ARTICLE

Atomistic Model of Uranium

Ru-song Li*, Bing He, Quan-hu Zhang

Xi'an Research Institute of Hi-Tech, Xi'an 710025, China

(Dated: Received on January 27, 2011; Accepted on May 18, 2011)

The electronic state and potential data of U_2 molecules are performed by first principle calculations with B3LYP hybrid exchange-correlation functional, the valence electrons of U atom are treated with the (5s4p3d4f)/[3s3p2d2f] contraction basis sets, and the cores are approximated with the relativistic effective core potential. The results show that the ground electronic state is $X^9\Sigma_g^+$. The pair potential data are fitted with a Murrell-Sorbie analytical potential function. The U-U embedded atom method (EAM) interatomic potential is determined based on the generalized gradient approximation calculation within the framework of the density functional theory using Perdew-Burke-Ernzerhof exchange-correlation functional at the spin-polarized level. The physical properties, such as the cohesive energy, the lattice constant, the bulk modulus, the shear modulus, the sc/fcc relative energy, the hcp/fcc relative energy, the shear modulus and the monovacancy formation energy are used to evaluate the EAM potential parameters. The U-U pair potential determined by the first principle calculations is in agreement with that defined by the EAM potential parameters. The EAM calculated formation energy of the monovacancy in the fcc structure is also found to be in close agreement with DFT calculation.

Key words: First principles, Embedded atom method, Multiplicity, Molecular dynamics

I. INTRODUCTION

Plutonium metallurgy lies at the heart of the scientific challenges to the nuclear stockpile. Aging mechanisms based on the atomic level are essential to assess the security and reliability of the weapon grade (WG) Pu materials. δ -Pu has been used since Manhattan project for nuclear explosives [1, 2]. He atoms released by Pu α decay accumulate in the form of He bubble, which will lead to volumetric expansion. Vacancies and self-interstitial atoms (SIA) produced by U displacement cascade will diffuse in the lattice, recombine with each other, or form vacancy or SIA cluster, these defects will cause macroscopic changes, such as decreasing density, dimension expansion, and creeping [3–8]. Wolfer *et al.* investigated the evolution for lattice parameter of Ga-stabilized δ -Pu alloy, the volume expansion, and the effect of pressure on the phase stability of Pu-Ga alloy system during self-irradiation, or aging by X-ray diffraction, dilatometer, and isochronal annealing technique, and they observed that sample occurred $\delta \rightarrow \alpha'$ Martensitic transition [9–15].

Many excellent reports focused on the displacement cascade evolution of 85 keV U recoil nucleus produced by ^{239}Pu α decay [8, 16–20], the point defects (such as vacancy, SIA, and their clusters) microstructural con-

figurations, and recombination behaviors. Other researchers had investigated the He-vacancy cluster and the three-dimensional He bubble nucleation [21–24], the volumetric swelling induced by the defect clusters, remnants of the large collision cascades that the U recoils produce, He bubbles, and the voids. While other groups had paid more attention on the Pu-Ga phase diagram, especially the $\delta \rightarrow \alpha'$ Martensitic transition at subambient temperature in Pu alloys, and the lattice parameters and the volumetric swelling as a function of the Ga atomic content during the aging of Pu-Ga alloys [1, 7, 9, 12]. However, little attention is paid on effect of the U recoil nucleus on the physical properties (such as swelling and lattice parameters) and phase stability. Pu-Pu, Pu-U, and U-U interatomic potentials are the key parameters for performing the molecular dynamics (MD) simulations of these effects. Pu-Pu interatomic potential can be described by the modified embedded atom method (MEAM) potential of Baskes *et al.* [25]. In our previous work, the EAM interatomic potential for Pu-U system has been constructed based on the first principle calculations [26]. In the present work, we plan to develop the U-U EAM potential by using the same methods.

II. METHODOLOGY

In MEAM formalism, the total energy E of a system of monatomic atoms has been given by an approximation of the form [27–29].

* Author to whom correspondence should be addressed. E-mail: rusong231@126.com

$$E = \sum_i \left[F(\bar{\rho}_i) + \frac{1}{2} \sum_{j \neq i} \Phi(R_{ij}) \right] \quad (1)$$

where the embedding function F is the energy to embed an atom of type i into the background electron density at site i , and Φ is the pair interaction between atoms i and j whose separation is given by R_{ij} . The embedding energy is given by

$$F_i(\bar{\rho}_i) = A_i E_i^0 \frac{\bar{\rho}_i}{\rho_0} \ln \frac{\bar{\rho}_i}{\rho_0} \quad (2)$$

where the sublimation energy E_i^0 and parameter A_i depend on the element type of atom i . ρ_0 is the scaling factor for the background electron density (in fcc structure material, $\rho_0 = Z_1 = 12$). The background electron density $\bar{\rho}_i$ is given in Eqs. (3) and (4)

$$\bar{\rho}_i = \rho^{(0)} (1 + \Gamma)^{1/2} \quad (3)$$

$$\bar{\rho}_i = \rho^{(0)} \frac{2}{1 + \exp(-\Gamma)} \quad (4)$$

For the actinide elements, such as Pu and U, narrower 5f bands along with properties intermediate between those of localized 4f and delocalized 3d orbitals, near the Fermi level, are believed to be responsible for the exotic structure of actinides under ambient condition [30]. For the light actinides with delocalized 5f electrons, the behavior is well described with standard DFT. At the present time, the appropriate methods for dealing with U and U alloys are the hybrid exchange-correlation functional (such as B3LYP, PBE0), the self-interaction correction (SIC), the dynamics mean field theory (DMFT), the local density approximation (LDA), or the generalized gradient approximation (GGA) [31, 32].

For U-U pair potential, potential data can be obtained from first principle calculation. According to the atomic and molecular reaction statics (AMRS) [33], U atom belongs to group SO(3). The irreducible representations of the ground electronic states of U atom is 5L_u , and it can be resolved into that of U_2 (group $D_{\infty h}$) as follows:

$$U: ^5L_u \rightarrow ^5\Sigma_u^- \oplus ^5\Pi_u \oplus ^5\Delta_u \oplus ^5\Phi_u \oplus ^5\Gamma_u \oplus \dots$$

$$\begin{aligned} \text{So the possible electronic states for } U_2 \text{ molecule are} \\ ^5L_u \otimes ^5L_u = (& ^5\Sigma_u^- \oplus ^5\Pi_u \oplus ^5\Delta_u \oplus ^5\Phi_u \oplus ^5\Gamma_u \oplus \dots) \otimes \\ & (^5\Sigma_u^- \oplus ^5\Pi_u \oplus ^5\Delta_u \oplus ^5\Phi_u \oplus ^5\Gamma_u \oplus \dots) \\ = & ^{1,3,5,7,9}\Sigma_g^+ (5), ^{1,3,5,7,9}\Pi_g (6), ^{1,3,5,7,9}\Delta_g (5), \\ & ^{1,3,5,7,9}\Phi_g (5), ^{1,3,5,7,9}\Gamma_g (5), ^{1,3,5,7,9}\Sigma_g^- (3), \\ & ^{1,3,5,7,9}H_g (2), ^{1,3,5,7,9}I_g (2) \dots \end{aligned}$$

In the first principle calculations for U-U pair potentials, the valence electrons of U atom can be treated with the (5s4p3d4f)/[3s3p2d2f] contraction basis set, and the core is approximated with the relativistic effective core potential (RECP). The U-U pair potential data are predicted with Becke-3 hybrid exchange-correlation functional (B3LYP) implemented in the

Gaussian 09w code [34–37], then they can be fitted with the following modified Murrell-Sorbie analytical potential function. The convergence of self-consistent field (SCF) is less than 10^{-8} .

$$\Phi(R) = -D_e \left(1 + \sum_{l=1}^n a_l d^l \right) \exp(-a_1 d) \quad (5)$$

where D_e is the dissociation energy, $d = r - r_0$, r is the interatomic distance, r_0 is the equilibrium interatomic distance, a_l and n are potential function parameters.

The cohesive energies E_c of U atoms in various structures can be defined as [38]

$$E_c = \frac{E_{\text{tot}} - N E_{\text{atom}}}{N} \quad (6)$$

where E_{tot} is the total energy of the system, N is the number of U atoms in the system, and E_{atom} is the total energy of an isolated U atom.

For the spin-orbit coupling (SOC) effect, the electronic and geometric properties of actinide complexes without treating spin-orbit effects could be adequately described [39–43]. So the effect of spin-orbit coupling is omitted in this work. The DFT calculations for U atoms in various crystal structures are performed by $10 \times 10 \times 10$ Monkhorst-Pack grids and the improved tetrahedron method with Gaussian smearing (0.1 eV) under the generalized gradient approximation (GGA) using Perdew-Burke-Ernzerhof (PBE) exchange-correlation functional at the spin-polarized (SP) level within the projected augmented wave (PAW) method as implemented in the ABINIT code [44]. This package is based on an efficient fast Fourier transform algorithm for the conversion of wave functions between real and reciprocal space, on the adaptation to a fixed potential of the band-by-band conjugate-gradient method [45], and on a potential-based conjugate-gradient algorithm for the determination of the self-consistent potential. A plane-wave cutoff energy $E_{\text{cut}} = 400$ eV is chosen. The core of U atom is approximated with the ultra-soft pseudopotential (USPP). The convergence of self-consistent field (SCF) is less than 0.01 meV/atom. Nonmagnetic configuration is appropriate for light actinide-U element from the point of total energy, so the U5f electrons in this work are in delocalized 5f³ electronic configuration.

The formula for the monovacancy formation energy without any structural relaxations in a bcc/fcc supercell containing 16/32 atoms is given by [46]

$$E_f^{1v} = E_{N-1} - \frac{N-1}{N} E_N \quad (7)$$

where E_N is the total energy of an N -atom unit cell.

During the modeling of U-U EAM potential, the total energy per atom for the equilibrium reference structure is obtained from the 0 K universal equation of state

(EOS) of Rose *et al.* [47] as a function of nearest-neighbor distance,

$$F[\bar{\rho}^0(R)] + \frac{1}{2} \sum \Phi(R) = E^u(R) \\ = -E_c \left(1 + a^* + \delta \frac{r_e}{R} a^{*3} \right) e^{-a^*} \quad (8)$$

$$a^* = \alpha \left(\frac{R}{r_e} - 1 \right) \quad (9)$$

$$\alpha = \sqrt{\frac{9B\Omega}{E_c}} \quad (10)$$

where $E^u(R)$ is the universal function for a uniform expansion or contraction in the reference structure, r_e is the equilibrium nearest neighbor distance, B is the bulk modulus, α is the exponential decay factor for the 0 K universal Rose EOS, and Ω is the equilibrium atomic volume. δ is a parameter related to the pressure derivative of the bulk modulus of the reference phase. If only first nearest-neighbor interactions are considered in the EAM, the total energy per atom can be given by

$$E^u(R) = F[\bar{\rho}^0(R)] + \frac{Z_1}{2} \Phi(R) \quad (11)$$

where Z_1 is the number of nearest-neighbor atoms. The expressions for the embedding energy $F[\bar{\rho}^0(R)]$ and the total energy per atom $E^u(R)$ are obtained from the Eqs. (2) and (8), respectively. Because the local environment for individual U atom is similar, the expression for the pair potential between two atoms separated by a distance R is obtained from Eq.(11) as follows:

$$\Phi(R) = \frac{2}{Z_1} \{ E^u(R) - F[\bar{\rho}^0(R)] \} \quad (12)$$

and it can be compared with the pair potential definition in Eq.(5).

A , $\beta^{(0)}$, $\beta^{(2)}$, and $t^{(2)}$ are iterated from the following equations [46], A is the scaling factor for the embedding energy.

$$A = \frac{-E_c + \delta E_{sc} + 0.5E_c(1 + a_{sc}^*)e^{-a_{sc}^*}}{0.5E_c \ln(0.5)e^{-b_{sc}^*}} \quad (13)$$

$$c_{44} = \frac{E_c}{\Omega} \left[\frac{\alpha^2 - A\beta^{(0)2}}{Z} + \frac{2At^{(2)}(\beta^{(2)} - 2)^2}{Z^2} \right] \quad (14)$$

$$c_{11} - c_{12} = \frac{E_c}{\Omega} \left[\frac{\alpha^2 - A\beta^{(0)2}}{Z} + \frac{At^{(2)}(\beta^{(2)} - 6)^2}{Z^2} \right] \quad (15)$$

$$a_{sc}^* = \alpha(x_{sc} - 1) \quad (16)$$

$$b_{sc}^* = \beta^{(0)}(x_{sc} - 1) \quad (17)$$

The ratio of nearest distances in the sc structure to the fcc structure is given by

$$x_{sc} = \frac{\sqrt{2}}{4^{1/3}} \quad (18)$$

The elastic constants C_{11} , C_{12} , and C_{44} are the calculated results of the fcc phase. Johnson found that

the electron density decay constant equaling 6.0 in fcc structure yielded reasonable results [48], so we chose 6.0 for $\beta^{(2)}$.

The relative energy of hcp and fcc is used to determine $t^{(3)}$

$$\Delta E_{\text{hcp}} = F(\bar{\rho}_{\text{hcp}}) \quad (19)$$

$$\bar{\rho}_{\text{hcp}} = \sqrt{Z_1^2 + \frac{1}{3}t^{(3)}} \quad (20)$$

The monovacancy formation energy in bcc structure is used to determine $t^{(1)}$

$$E_f^{1v} = E_c + Z_1 F(\bar{\rho}_v) \quad (21)$$

$$\bar{\rho}_v = \sqrt{(Z_1 - 1)^2 + t^{(1)} + \frac{2}{3}t^{(2)} + \frac{2}{5}t^{(3)}} \quad (22)$$

Angular screening was implemented using the nominal values, $C_{\text{min}}=1.4$ and $C_{\text{max}}=2.8$ [49, 50].

III. RESULTS AND DISCUSSION

A. U-U pair potential

As discussed above, the multiplicities of U_2 are 1, 3, 5, 7, and 9, the unpaired electrons are 0, 2, 4, 6, and 8, respectively. Because of U 5f electrons hybrid with 6d electrons and the configuration mixture effect, the outer-shell orbits may be the multiple contributions from 5f electrons, 7s electrons, and other electrons. The electronic states are undetermined, initial guess orbital changes in the calculation, so we predict several minimum potentials.

When the multiplicity of U_2 molecule is 9, and U-U interatomic distance is 0.33 nm, U_2 molecule is the most stable, so the electronic state for the ground state is $X^9\Sigma_g^+$. The Murrell-Sorbie analytical potential function is used to fit the potential data with regular equations, the disassociation energies $D_e=565.58$ meV, the equilibrium interatomic distance $r_o=0.33$ nm, and $a_1, a_2, a_3, a_4, a_5, a_6$ are 7.177 nm^{-1} , -243.1 nm^{-2} , 93.89 nm^{-3} , -2377 nm^{-4} , 5027 nm^{-5} , -7366 nm^{-6} , respectively. The calculation result of Pepper *et al.* [51] shows that the ground electronic state of U_2 is an $X^5\Sigma_g^+$ state, this state is in fact a metastable state according to our previous work, which is in accordance with the work of Gagliardi *et al.* [52].

Our present result is different from the work of Gagliardi *et al.*, D_e and r_o are 1.32 eV and 0.24 nm, respectively [52]. The possible reasons for this discrepancy are that we adopt the relativistic effective core potential (RECP) to replace the electrostatic potential between the nucleus and the electrons, and the internucleus orthogonal effect based on the Born-Oppenheimer (OB) approximation. The relativistic effects of orbital extension and contraction, the terms of "mass-velocity" and "Darwin" are also considered. The self-energy of

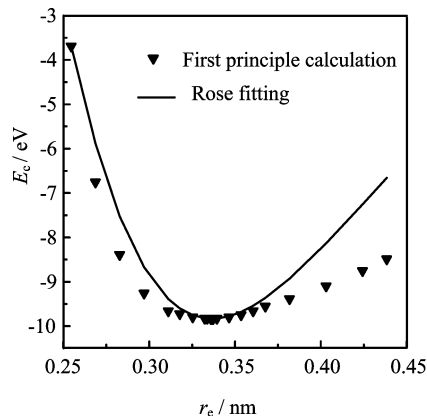


FIG. 1 The cohesive energies as a function of the nearest distance for U atoms in fcc crystal structure compared with the curve fitted from the Rose equation.

TABLE I Comparison of GGA+SP results for fcc, α and γ phase U with the experimental values.

	C_{11}/GPa	C_{12}/GPa	C_{44}/GPa	B/GPa	Ω/nm^3
fcc U	59.0	34.5	10.2	135.0	0.0202
γ -U	103.9	120.1	30.7	114.7	0.0192
α -U	305.0	82.2	-121.9	148.6	0.0195
Expt.	214.7	46.5	124.4	113.0	0.0208

valence orbital is regenerated in the RECP approximation, the core orbitals and the valence orbitals are given by the relativistic Cowan-Griffin Hartree-Fock equation, so the calculation is much more efficient than the full electronic calculation. However, Gagliardi *et al.* used a basis set of the atomic natural orbital (ANO) type that has been developed especially for relativistic calculations with the Douglas-Kroll-Hess (DKH) Hamiltonian. A primitive set 26s23p17d13f5g was contracted to 9s8p7d5f2g. A larger ANO basis set was constructed for the calculation of the binding energy, in which the primitive set 27s24p18d14f6g3h was contracted to 11s10p8d6f3g1h, so they gave a more precise result.

B. Potential parameters

The elastic constants (C_{11} , C_{12} , and C_{44}) and the bulk modulus B for orthogonal α -U (space group $Cmcm$), tetragonal β -U (space group $P4_2nm$) and bcc γ -U (space group $Im3m$) are calculated with GGA+PBE at the spin-polarized (SP) level. For U element, all f electrons are treated as itinerant (delocalized 5f electrons in f^3 configuration). The calculated electronic structure is in agreement with the earlier work [53]. Large change in electron coupling behavior is due to the delocalized nature of the 5f states in U compared to the localized nature of the 5f states in Pu [54]. The calculated physical properties are listed in Table I. All the calculated bulk modulus and the atomic volumes

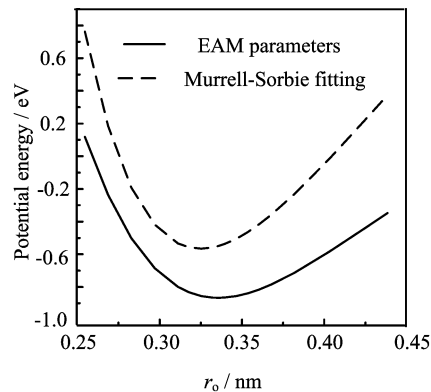


FIG. 2 Murrell-Sorbie fitted and EAM parameters determined values of U-U pair potential as a function of U-U interatomic distance.

are in agreement with the experiment values [55].

The U-U EAM parameters are obtained by using DFT data for U atom with the fcc reference lattice structure. The sources of the DFT calculation data and the potential parameter values are listed in Table II. E_c , r_e , α , and δ are determined by Rose fitting of cohesive energy/nearest distance in fcc structure, as shown in Fig.1 and Table II. From Table II we can see that $\delta < 0$, so the third-order term in universal Rose EOS (Eq.(8)) softens the repulsive branch of interatomic potential, while hardens the attractive branch of interatomic potential.

C. Verification of potential parameters

The Murrell-Sorbie fitting result is in agreement with the definition in Eq.(12), as shown in Fig.2.

To test the validity of the U-U EAM potential parameters, the cohesive energies of U atoms in sc (space group Pm3m), bcc (space group Im3m), and hcp (space group $P6_3/mmc$, the lattice parameter c/a ratio is fixed at the ideal value) crystal structures for different lattice constants are calculated, and compared with those of DFT calculations in Fig.3 and Fig.4. Interestingly, the predicted equilibrium interatomic distance of U_2 molecule $r_o=0.33$ nm is consistent with the nearest distance of fcc structure U $r_e=0.3658$ nm (as shown in Table II and Fig.1), and that of bcc γ phase U $r_e=0.32476$ nm (as shown in Fig.3). The agreements between EAM potential and DFT calculation results for the bcc and the hcp structures are also very obvious, although the EAM result for the sc structure is slightly overestimated. The total energies per atom in various structures are also consistent with the DFT calculations. It should be noted that EAM potential evaluation result (0.02 nm^3) also reproduces the experimental volume (0.0208 nm^3).

To compare the monovacancy formation energy evaluated by the U-U EAM potential with the corresponding formation energy predicted by DFT method.

TABLE II The sources of the DFT calculation data and the parameter values.

Parameter ^a	Source	Value
E_c/eV	Cohesive energy of fcc structure	9.8295
r_e/nm	Lattice constant of fcc structure	0.3366
α (dimensionless)	Bulk modulus of bcc structure	3.6727
A (dimensionless)	Relative energy of sc and fcc structures	1.2858
$\beta^{(0)}$ (dimensionless)	Shear modulus of fcc structure	2.7387
$\beta^{(1)}$ (dimensionless)	Nominal value	1.00
$\beta^{(2)}$ (dimensionless)	Shear modulus of fcc structure	6.00
$\beta^{(3)}$ (dimensionless)	Nominal value	1.00
$t^{(1)}$ (dimensionless)	Monovacancy formation energy in bcc structure	-0.2090
$t^{(2)}$ (dimensionless)	Shear modulus of fcc structure	-0.6533
$t^{(3)}$ (dimensionless)	Relative energy of hcp and fcc structures	23.7570
δ (dimensionless)	Rose fitting of cohesive energy/nearest distance in fcc structure	-0.0512

^a $\beta^{(0)-(3)}$ are the exponential decay factors for the atomic densities, $t^{(0)-(3)}$ are the weighting factors for the atomic densities.

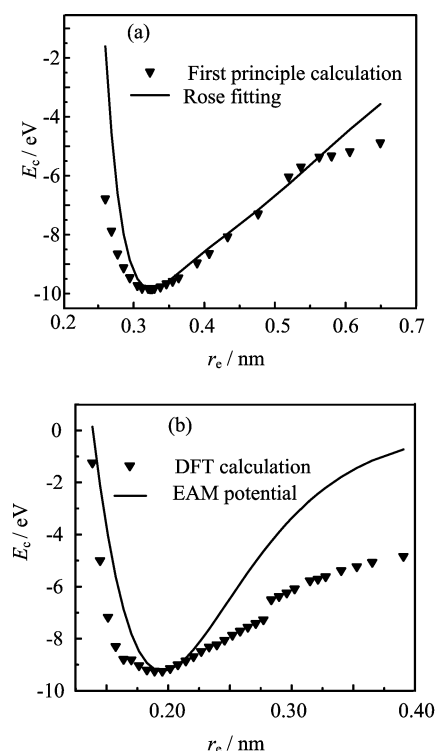


FIG. 3 The cohesive energies obtained from the EAM potential as a function of (a) the nearest distance for U atoms in bcc structure, (b) the nearest distance for U atoms in sc structure, which are compared with the DFT calculation.

$10a_0 \times 10a_0 \times 10a_0$ periodic supercell is completely relaxed in the canonic ensemble (NVT), where a_0 is the lattice constant of fcc U. The monovacancy configuration is realized by removing an arbitrary atom from the cell, so the monovacancy formation energy is the mean value averaged over several geometric relaxation

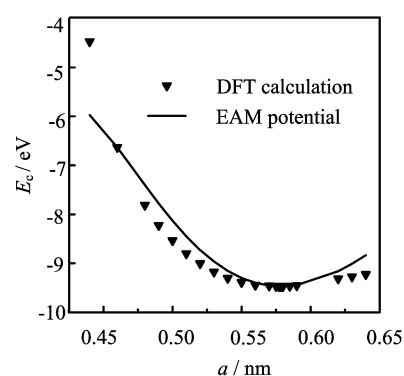


FIG. 4 The cohesive energies obtained from the EAM potential as a function of the lattice constant a for U atoms in hcp structure, which are compared with the DFT calculation.

results. Six-order Gear predictor-corrector algorithm and Nose-Hoover thermostat are employed, the total simulation time is 20 ps, and the time step is 1 fs. Angular screening was implemented using $C_{\min}=1.4$ and $C_{\max}=2.8$, a radial cutoff distance of 0.476 nm is also used. Because of the many-body screening effects, the calculation results are independent from radial cutoff distances, as far as they are larger than the second nearest neighbor. The convergence of total energy is less than 0.01 meV. The monovacancy formation energy E_{vf} in the fcc structure based on DFT method is calculated at the GGA+SP level, we find that the EAM potential give a result ($E_{vf}=2.320$ eV) in good agreement with DFT calculation result ($E_{vf}=1.927$ eV).

IV. CONCLUSION

In this work the electronic states and potential data of U_2 molecules are performed by the first principle

calculations with B3LYP hybrid exchange-correlation functional. The results show that the ground electronic state is $X^9\Sigma_g^+$. The pair potential data are fitted with a modified Murrell-Sorbie analytical potential function. The U-U interatomic potential parameters are determined based on the DFT calculation results and the embedded atom method (EAM). The U-U pair potential determined by the first principle calculations is in agreement with that defined by the EAM potential parameters. The reliability and the flexibility of the EAM potential parameters have been tested for U atoms in bcc, sc, and hcp structure. In the future work, we plan to adopt Pu-Pu, Pu-U and U-U potential to perform MD calculation of the effects of U recoil nucleus on the material properties, such as the volumetric expansion, the lattice parameters, the elastic constants, and the phase stability in δ -Pu. MD results along with the point defects properties, such as the migration energies, the formation energies and the mobilities can be used as the input data of the mesoscopic Monte Carlo and the rate equations simulations.

V. ACKNOWLEDGMENT

We would like to thank W. Li for useful discussion.

- [1] N. Baclet, B. Oudot, R. Grynszpan, L. Jolly, B. Ravat, P. Faure, L. Berlu, and G. Jomard, *J. Alloys Compd.* **444-445**, 305 (2007).
- [2] S. H. Siegfried, *Metall. Mater. Trans. A* **39**, 1585 (2008).
- [3] B. Y. Ao, X. L. Wang, W. Y. Hu, J. Y. Yang, and J. X. Xia, *J. Alloys Compd.* **444-445**, 300 (2007).
- [4] W. G. Wolfer, B. Oudot, and N. Baclet, *J. Nucl. Mater.* **359**, 185 (2006).
- [5] M. J. Caturla, T. D. de la Rubia, and M. Fluss, *J. Nucl. Mater.* **323**, 163 (2003).
- [6] B. W. Chung, S. R. Thompson, K. E. Lema, D. S. Hiramoto, and B. B. Ebbinghaus, *J. Nucl. Mater.* **385**, 91 (2009).
- [7] B. W. Chung, S. R. Thompson, C. H. Woods, D. J. Hopkins, W. H. Gourdin, and B. B. Ebbinghaus, *J. Nucl. Mater.* **355**, 142 (2006).
- [8] M. Robinson, S. D. Kenny, R. Smith, M. T. Storr, and E. McGee, *Nucl. Instr. Meth. B* **267**, 2967 (2009).
- [9] W. G. Wolfer, A. Kubota, P. Söderlind, A. I. Landa, B. Oudot, B. Sadigh, J. B. Sturgeon, and M. P. Surh, *J. Alloys Compd.* **444-445**, 72 (2007).
- [10] S. S. Hecker and J. C. Martz, *Los Alamos Sci.* **26**, 238 (2000).
- [11] F. J. Freibert, D. E. Dooley, and D. A. Miller, *J. Alloys Compd.* **444-445**, 320 (2007).
- [12] B. Ravata, B. Oudot, and N. Baclet, *J. Nucl. Mater.* **366**, 288 (2007).
- [13] W. G. Wolfer, P. Söderlind, and A. Landa, *J. Nucl. Mater.* **344**, 21 (2006).
- [14] M. J. Fluss, B. D. Wirth, M. Wall, T. E. Felter, M. J. Caturla, A. Kubota, and T. Diaz de la Rubia, *J. Alloys Compd.* **368**, 62 (2004).
- [15] D. R. Harbur, *J. Alloys Compd.* **444-445**, 249 (2007).
- [16] P. Pochet, *Nucl. Instr. Meth. B* **202**, 82 (2003).
- [17] S. M. Valone, M. I. Baskes, M. Stan, T. E. Mitchell, A. C. Lawson, and K. E. Sickafus, *J. Nucl. Mater.* **324**, 41 (2004).
- [18] G. Jomard, L. Berlu, G. Rosa, P. Faure, J. Nadal, and N. Baclet, *J. Alloys Compd.* **444-445**, 310 (2007).
- [19] L. Berlu, G. Jomard, G. Rosa, and P. Faure, *J. Nucl. Mater.* **374**, 344 (2008).
- [20] S. I. Samarin and V. V. Dremov, *J. Nucl. Mater.* **385**, 83 (2009).
- [21] B. P. Uberuaga and S. M. Valone, *J. Nucl. Mater.* **375**, 144 (2008).
- [22] B. P. Uberuaga, S. M. Valone, and M. I. Baskes, *J. Alloys Compd.* **444-445**, 314 (2007).
- [23] S. M. Valone, M. I. Baskes, and R. L. Martin, *Phys. Rev. B* **73**, 214209 (2006).
- [24] D. W. Wheeler and P. D. Bayer, *J. Alloys Compd.* **444-445**, 212 (2007).
- [25] M. I. Baskes, *Phys. Rev. B* **62**, 15532 (2000).
- [26] R. S. Li, B. He, and Q. H. Zhang, *Nucl. Sci. Tech.* **22**, 47 (2011).
- [27] M. S. Daw and M. I. Baskes, *Phys. Rev. B* **29**, 6643 (1984).
- [28] M. S. Daw and M. I. Baskes, *Phys. Rev. Lett.* **50**, 1285 (1983).
- [29] M. I. Baskes, *Phys. Rev. B* **46**, 2727 (1992).
- [30] R. A. Fynn and A. K. Ray, *Phys. Rev. B* **75**, 195112 (2007).
- [31] G. Jomard, B. Amadon, and F. Bottin, *Phys. Rev. B* **78**, 075125 (2008).
- [32] S. Y. Savrasov and G. Kotliar, *Phys. Rev. Lett.* **84**, 3670 (2000).
- [33] Z. H. Zhu, *Atomic and Molecular Reaction Statics*. Beijing: Science Press, 56 (2007).
- [34] A. D. Becke, *J. Chem. Phys.* **98**, 5648 (1993).
- [35] C. Lee, W. Yang, and R. G. Parr, *Phys. Rev. B* **37**, 785 (1988).
- [36] P. J. Hay and R. L. Martin, *J. Chem. Phys.* **109**, 3875 (1998).
- [37] M. J. Frisch, G. W. Trucks, H. B. Schlegel, G. E. Scuseria, M. A. Robb, J. R. Cheeseman, J. A. Montgomery Jr., T. Vreven, K. N. Kudin, J. C. Burant, J. M. Millam, S. S. Iyengar, J. Tomasi, V. Barone, B. Mennucci, M. Cossi, G. Scalmani, N. Rega, G. A. Petersson, H. Nakatsuji, M. Hada, M. Ehara, K. Toyota, R. Fukuda, J. Hasegawa, M. Ishida, T. Nakajima, Y. Honda, O. Kitao, H. Nakai, M. Klene, X. Li, J. E. Knox, H. P. Hratchian, J. B. Cross, C. Adamo, J. Jaramillo, R. Gomperts, R. E. Stratmann, O. Yazyev, A. J. Austin, R. Cammi, C. Pomelli, J. W. Ochterski, P. Y. Ayala, K. Morokuma, G. A. Voth, P. Salvador, J. J. Dannenberg, V. G. Zakrzewski, S. Dapprich, A. D. Daniels, M. C. Strain, Ö. Farkas, D. K. Malick, A. D. Rabuck, K. Raghavachari, J. B. Foresman, J. V. Ortiz, Q. Cui, A. G. Baboul, S. Clifford, J. Cioslowski, B. B. Stefanov, G. Liu, A. Liashenko, P. Piskorz, I. Komaromi, R. L. Martin, D. J. Fox, T. Keith, M. A. Al-Laham, C. Y. Peng, A. Nanayakkara, M. Challacombe, P. M. W. Gill, B. Johnson, W. Chen, M. W. Wong, C. Gonzalez, and J. A. Pople, *Gaussian 09 Package.*, Pittsburgh PA: Gaussian Inc., (2009).
- [38] B. Jelinek, J. Houze, Sungho Kim, M. F. Horstemeyer,

- M. I. Baskes, and S. Gon Kim, *Phys. Rev. B* **75**, 054106 (2007).
- [39] Y. Wang and Y. Sun, *J. Phys.: Condens. Mater.* **12**, L311 (2000).
- [40] A. Landa and B. Sadigh, *Phys. Rev. B* **66**, 205109 (2002).
- [41] L. Vitos, J. Kollar, and H. L. Skriver, *Phys. Rev. B* **55**, 4947 (1997).
- [42] J. Kollar, L. Vitos, and H. L. Skriver, *Phys. Rev. B* **55**, 15353 (1997).
- [43] P. J. Hay and R. L. Martin, *J. Chem. Phys.* **109**, 3875 (1998).
- [44] F. Jollet, G. Jomard, and B. Amadon, *Phys. Rev. B* **80**, 235109 (2009).
- [45] M. Torrent, F. Jollet, F. Bottin, G. Zérah, and X. Gonze, *Comput. Mater. Sci.* **42**, 337 (2008).
- [46] M. I. Baskes, S. P. Chen, and F. J. Cherne, *Phys. Rev. B* **66**, 104107 (2002).
- [47] J. H. Rose, J. R. Smith, F. Guinea, and J. Ferrante, *Phys. Rev. B* **29**, 2963 (1984).
- [48] R. A. Johnson, *Phys. Rev. B* **37**, 3924 (1988).
- [49] M. I. Baskes, J. E. Angelo, and C. L. Bisson, *Modell. Simul. Mater. Sci. Eng.* **2**, 505 (1994).
- [50] M. I. Baskes, *Mater. Chem. Phys.* **50**, 152 (1997).
- [51] M. Pepper and B. E. Bursten, *J. Am. Chem. Soc.* **112**, 7803 (1990).
- [52] L. Gagliardi and B. O. Roos, *Nature* **433**, 848 (2005).
- [53] M. D. Jones and R. C. Albers, *Phys. Rev. B* **79**, 045107 (2009).
- [54] K. T. Moore, G. van der Laan, R. G. Haire, M. A. Wall, and A. J. Schwartz, *Phys. Rev. B* **73**, 033109 (2006).
- [55] E. S. Fisher and H. J. Mcskimin, *J. Appl. Phys.* **29**, 1473 (1958).